

Superresonant Radiation Stimulated by Higher Harmonics

Cristian Redondo Lourés, Thomas Roger, Daniele Faccio, and Fabio Biancalana

School of Engineering and Physical Sciences, Heriot-Watt University, EH14 4AS Edinburgh, United Kingdom

(Received 18 August 2016; published 27 January 2017)

Solitons propagating in media with higher-order dispersion will shed radiation known as resonant radiation, with applications in frequency broadening, deep UV sources for spectroscopy, and fundamental studies of soliton physics. Using a recently proposed equation that models the behavior of ultrashort optical pulses in nonlinear media using the analytic signal, we find that the resonant radiation associated with the third-harmonic generation term of the equation is parametrically stimulated with an unprecedented gain. Resonant radiation levels, typically only a small fraction of the soliton, are now as intense as the soliton itself. The mechanism is universal and works also in normal dispersion and with harmonics higher than the third. We report experimental hints of this superresonant radiation stimulated by the fifth harmonic in diamond.

DOI: 10.1103/PhysRevLett.118.043902

Introduction.—The process of resonant radiation emission in nonlinear media is extremely general and has been studied in many different systems, like solitons in fibers and bulk media [1–6], 3D light bullets [7–9], dispersive shock waves [10], resonators [11–15], and complex scenarios combining a mixture of the above [16]. This emission is dictated by a nonlinear momentum conservation; i.e., the requirement is that the momentum of the pump is equal to the linear momentum of the dispersive wave propagating in normal dispersion [2,4,5]—known as the *phase-matching condition*. For a system governed by the nonlinear Schrödinger equation (NLSE), it can only occur when a third (or higher) order dispersion term is present. In a recent work, Conforti *et al.* proposed an equation for the *analytic signal* of an electric field that is formally similar to the NLSE but does not suffer from many of the limitations of the latter [17] and only relies on the reasonable assumption of neglecting backward propagating waves [18]. This equation has been found to predict features of the nonlinear interaction between light and matter that were not present in the original NLSE, related to the so-called negative-frequency components of the pulse [19–23]. In Ref. [17] the authors discuss new phase-matching conditions that arise from the new nonlinear polarization terms in their equation, and they theoretically predict the emission of the so-called negative resonant radiation (NRR) and third-harmonic resonant radiation (THRR). The former had been previously identified experimentally by Rubino *et al.* [19]; see also Ref. [24]. However, the new THRR term was located in the deep infrared region of the spectrum for the system analyzed (fused silica), where it was not efficiently fed by the pump and thus has never been observed.

In this Letter we explore the possibility of promoting the THRR signal into a very strongly resonant mode. When the THRR frequency is close to a higher-harmonic frequency, a surprisingly large amount of the pump energy can be

transferred to the radiation via a *stimulated* process. This is a two step mechanism: the pump releases energy to a higher harmonic, and the higher-harmonic energy is then transferred to the resonant THRR mode. This mode then appears as a sharp, intense peak in the output spectrum. The surprising property of this novel radiation, which we dub *superresonant radiation* (SRR), is its extremely powerful gain dynamics and the unprecedented transfer of energy from the soliton to the radiation itself—setting the SRR apart from any currently known dispersive wave emission, with interesting potential uses in frequency conversion applications. In the final part, we show a clear experimental hint of SRR in diamond, where intense pulses in normal dispersion are used to excite the THRR, which is then promoted to SRR when its frequency is close to the *fifth* harmonic of the pump.

Governing equations.—The equation proposed by Conforti *et al.* [17] is, in dimensionless units,

$$i\partial_{\xi}A + \hat{D}(i\partial_{\tau})A + \left(1 + \frac{i}{\mu}\partial_{\tau}\right) \left[|A|^2A + |A|^2A^* \exp(2i\phi) + \frac{1}{3}A^3 \exp(-2i\phi) \right]_+ = 0, \quad (1)$$

where $A = A(\xi, \tau)$ is the envelope of the analytic signal of the electric field, ξ and τ are the dimensionless space and time variables (scaled with the second order dispersion length $L_D \equiv t_0^2/|\beta_2|$ and the input pulse duration t_0 , respectively), $\hat{D} \equiv \sum_{m=2}^{\infty} b_m (i\partial_{\tau})^m / m!$ is the dispersion operator, $b_m = \beta_m / (|\beta_2| t_0^{m-2})$ are the normalized dispersion coefficients, $\phi \equiv \kappa\xi + \mu\tau$, $\kappa \equiv (\beta_1\omega_0 - \beta_0)L_D$ is a crucial parameter that measures the difference between the group and phase velocities, $\mu = \omega_0 t_0$ is the normalized pulse frequency, β_1 is the inverse group velocity, β_0/ω_0 is the inverse phase velocity, $L_D \equiv t_0^2/|\beta_2|$ is the dispersion

length, and ω_0 is the central frequency of the pulse. Equation (1) has been successfully applied to optical fibers, crystals [17,21], and fiber or microring cavities [22].

The analytic signal $\mathcal{E} = A \exp(i\beta_0 z - i\omega_0 t)$ is the positive frequency part of the electric field E , which can be written as $E = (\mathcal{E} + \mathcal{E}^*)/2$, an equal mixture of positive and negative frequencies [20]. In the absence of nonlinear interactions, the fields \mathcal{E} and \mathcal{E}^* are completely decoupled, but the nonlinear polarization in Eq. (1) mixes both fields in a nontrivial way. The first term of the polarization inside the square brackets in Eq. (1) corresponds to the usual Kerr term. The third term is the third-harmonic generation, and the second is the so-called *negative-frequency Kerr term* [17]. The subscript $+$ in Eq. (1) means that spectral filtering must be performed since A must contain only the positive frequency components [17,21,22,25,26].

In Ref. [17] all of the phase-matching conditions for the emission of resonant radiations have been derived—there are *three* in total, one associated with each term of the nonlinear polarization:

$$D(\Delta) = 2m\kappa - (2m - 1)q, \quad (2)$$

where $q = 1/2$ is the normalized power of the incident pulse and $m = 1$ for NRR, $m = 0$ for the usual RR, and $m = -1$ for the THRR; see also Ref. [17]. $D(\Delta) = \sum_{n=2}^{\infty} b_n \Delta^n / n!$ is the Fourier transform of the dispersion operator, where Δ is the dimensionless detuning between pulse and radiation. Since, in experimentally accessible conditions, $\kappa \gg q$, if we are in deep anomalous dispersion ($b_2 < 0$ and all other dispersion coefficients can be ignored), $D(\Delta) \equiv b_2 \Delta^2 / 2 \leq 0$ and neither the phase matching for RR nor the one for NRR can be satisfied; see the blue solid curve in Fig. 1. However, the phase matching for THRR can be fulfilled for two values of the detuning, one positive and one negative (see the blue solid curve and the dots showing crossings in Fig. 1). In the same figure, we can see that when we include b_3 , all three phase-matching conditions can be satisfied for values of $\Delta > 0$, and there are three different detunings for which we expect

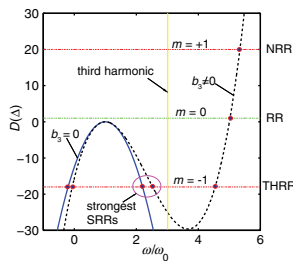


FIG. 1. Phase-matching curves from Eq. (2). The three horizontal lines represent the three phase-matching conditions: NRR (the upper, red line), RR (the medium, green line), and THRR (the lower, brown line). The two curves represent the dispersion for b_2 only (the blue, solid line) and $b_3 = 0.15$ (the black, dashed line). $\mu = 5$ and $\kappa = 10$ in both cases.

to find THRR; see the dashed black curve and the dots showing the crossings in Fig. 1.

We have numerically found that, when the position of the THRR is close to the third harmonic that is created by the pump as it propagates through the medium, the radiation will grow rapidly and appears as a narrow, very intense peak in the spectrum in the position predicted by the phase-matching condition (2), with $m = -1$. At variance with previously known dispersive wave emissions in fibers or bulk, this is a *two step mechanism*: the pulse gives energy to its third harmonic during propagation, and most of this energy is then transferred to the phase-matched THRR closest to the third-harmonic frequency. This last step can only occur if the THRR is spectrally located close to the third-harmonic frequency (see the purple oval in Fig. 1). We therefore say that the THRR has been “promoted” to SRR. This effect is extremely efficient: the third harmonic never manages to fully grow since the THRR continuously absorbs almost all of its energy, leading to the formation of an extremely intense and spectrally well-localized SRR peak. We have also checked to see that the possible emission of backward RR (which has its own phase-matching condition, and is far detuned and therefore very weak) is not detrimental to the formation of SRR [see also Fig. 6(c)].

Numerical simulations.—Figure 2 shows the evolution in the time domain of a sech pulse with $b_2 < 0$, $b_3 = 0$, $\mu = 5$, and $\kappa = 10$ after $\xi = 10$ dispersion lengths. These parameters are chosen in such a way that the THRR is phase matched at a frequency between the pump ($\omega/\omega_0 = 1$) and its third harmonic ($\omega/\omega_0 = 3$), around $\omega/\omega_0 \sim 2$. An oscillation appears on the top of the pulse in the time domain and then moves faster than the soliton, thus creating a leading oscillating tail. These violent intrasoliton oscillations are characteristic of the SRR.

The spectral evolution of this pulse is shown in Fig. 3. The spectrum develops a very intense peak at the position predicted for the THRR; see Eq. (2). This starts as a small

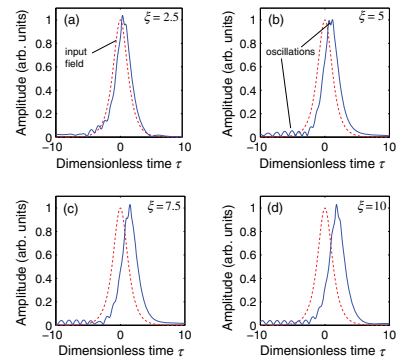


FIG. 2. Soliton in the time domain after a propagation of (a) $\xi = 2.5$, (b) 5, (c) 7.5, and (d) 10. We can see the oscillations on top of the pulse that leave it through the leading edge. The parameters are $b_3 = 0$, $\mu = 5$, and $\kappa = 10$.

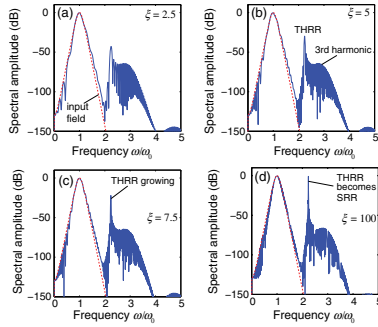


FIG. 3. Initial (red dashed line) and final (thick blue line) spectrum of a pulse after a propagation of (a) $\xi = 2.5$, (b) 5, (c) 7.5, and (d) 100, with other parameters as in Fig. 2. One can see the evolution of a THRR peak into a stimulated SRR, Eq. (2), for $m = -1$ (the vertical black dotted line).

peak in the third-harmonic peak but keeps growing with propagation, as energy is sucked from the third harmonic. Note that, for $\xi = 100$, this peak has grown to be more intense than the pump pulse. The THRR is parametrically stimulated by the third harmonic and is promoted to SRR. If the phase-matched THRR frequency is a bit outside the third-harmonic band, an important growth can still be observed; however, the THRR stimulation becomes increasingly weaker.

In Fig. 4 we show the XFROG spectrograms of the pulse evolution for $\xi = 2.5, 5, 7.5$, and 10, again for the case $b_3 = 0$. The third-harmonic radiation has two components, one that propagates alongside the pulse and another one leading it (“no. 1” and “no. 2,” respectively). The SRR extends between these two components of the third harmonic, confirming our hypothesis that SRR is THRR stimulated by higher harmonics.

When $b_3 = 0.15 \neq 0$, the situation changes significantly. As seen in Fig. 1, Eq. (2) predicts two (normally dispersive) phase-matched frequencies near the third harmonic (see the intersection between the black dashed line and the

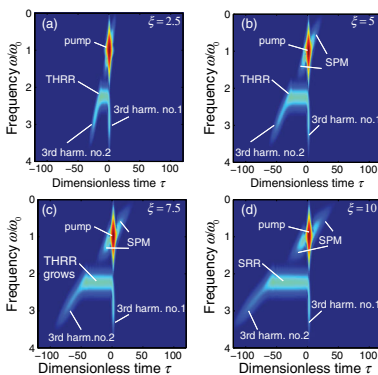


FIG. 4. XFROG for propagation lengths of (a) $\xi = 2.5$, (b) 5, (c) 7.5, and (d) 10. We can see the two components of the third harmonic described in the text and the SRR between them. Note how the SRR band grows indefinitely during the ξ evolution. SPM stand for self-phase modulation.

horizontal THRR line). Output spectra for the case $b_3 \neq 0$ are shown in Fig. 5. Two peaks appear at the positions predicted by the phase-matching conditions, with the one closer to the third-harmonic frequency growing much faster than the other. Again, the radiation peak closer to the third harmonic (which is inside the purple oval in Fig. 1) is a stimulated THRR which is then promoted to SRR.

Experimental hints of SRR.—We now show initial experimental evidence of THRR stimulated by the fifth harmonic in diamond. Odd harmonics higher than the third are generated in the sample during propagation due to cascaded four-wave mixing, for which the third-harmonic generation term of Eq. (1) is responsible. This term initially merges three photons of the pump with frequency ω_0 into a single photon with frequency $3\omega_0$, and then this secondary photon with two other photons of the pump, so that a pulse of frequency $5\omega_0$ is created. Therefore, we expect the resonant radiation coming from the third-harmonic term to be stimulated by any cascaded higher odd harmonic, albeit the resulting SRR would have smaller amplitude due to the decreasing intensity of higher harmonics. The use of the fifth harmonic instead of the third is useful in some materials due to the unclean spectra surrounding the third harmonic when pumping with very high energies. In diamond (normally dispersive) we cannot propagate solitons. The emissions in this case are *shock-front-assisted resonant radiations* [27]. The specific nature of the pulse generating the resonant emission is not important since the phase-matching conditions still hold. SRR is a general phenomenon that appears whenever a nonlinear system that exhibits cascaded higher-harmonic generation allows for resonant radiation associated with the higher-harmonic generation term (for a similar process occurring in $\chi^{(2)}$ media, see Refs. [28,29]).

We have used 50 fs pulses injected in a 500 μm bulk diamond. An amplified Ti:sapphire laser with the central wavelength $\lambda_0 = 785$ nm is used to pump an (OPA, TOPAS-C, Light Conversion Ltd.) producing infrared light pulses whose wavelength can be tuned between 1750 and 2050 nm, with a repetition rate of 100 Hz and a pulse duration of 70 fs. The IR pulses are focused with an $f = 150$ mm lens to a spot radius of ~ 36 μm providing a peak

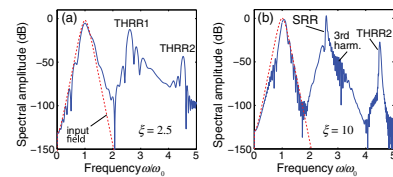


FIG. 5. Snapshots of the initial (red dashed line) and final (blue solid line) spectra during a propagation of (a) $\xi = 2.5$ and (b) $\xi = 10$ in the case $b_3 = 0.15$. The two vertical lines show the predicted position of the two THRRs. The THRR closer to the third-harmonic peak grows taller than the pump for $\xi = 10$, becoming a SRR. Other parameters are as in Fig. 2.

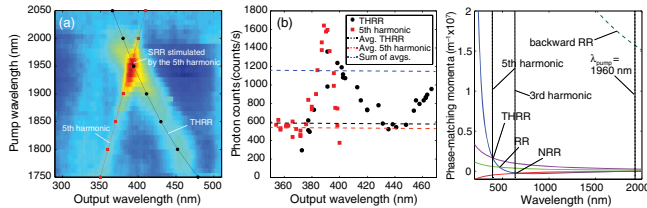


FIG. 6. (a) Emission of THRR (the black dots) and the fifth harmonic (the red squares) in diamond vs the pump wavelength. There is a crossing point of the THRR and fifth-harmonic emission for $\lambda_p \sim 1960$ nm. The SRR peak is generated at 390 nm. (b) THRR and fifth-harmonic peak maxima vs the pump wavelength. We find an enhancement of 40% compared to that predicted by taking the sum of the average values away from their overlapped wavelengths (the dashed red and black lines). (c) Phase-matching curves for all types of radiation in diamond.

intensity of $I = 28$ TW/cm². A single crystal diamond cut along the $\langle 100 \rangle$ axis is used to study the dynamics of the THRR vs the pump wavelength. The output of the diamond crystal is imaged onto a spectrometer (Andor Shamrock 303i spectrometer and iDus CCD camera) providing visible spectrum data. In order to isolate the fifth harmonic from the intense third-harmonic contribution and also have enough dynamic range, the high frequency component ($\lambda < 510$ nm) is blocked inside the spectrometer.

In Fig. 6(a) we show the high-energy part of the output spectrum after $L = 500$ μ m propagation when varying the input pulse wavelength from 1750 to 2050 nm. We can observe the fifth-harmonic peak shifting linearly towards longer wavelengths, as expected [see the red solid line and the red squares in Fig. 6(a), which shows the pump wavelength times 1/5]. However, an additional peak is observed which shifts towards shorter wavelengths when the pump wavelength is increased. The latter peak is due to THRR, as shown by the perfect agreement with the predicted THRR position [the black solid line and the black dots in Fig. 6(a)]. The prediction is based on the THRR phase-matching condition in normal dispersion and in the presence of the shock term, as in Ref. [27]. When the THRR and fifth-harmonic peaks have similar frequencies—i.e., when the pump wavelength is ~ 1960 nm—the THRR amplitude grows considerably, with a conversion efficiency larger than -50 dB from the pump. We have checked via an accurate phase-matching analysis to see that such enhancement is not due to a phase-matched, cascaded fifth-harmonic generation. The normal dispersion of diamond does not allow the formation of a soliton; i.e. the pulse intensity will quickly decrease in propagation; yet these results show that the phenomenon of SRR “promotion” is very general and relies only on the crossing of the THRR emission with a higher-order harmonic.

Figure 6(b) shows the peak intensities of the fifth harmonic and THRR taken along the red and black solid lines from Fig. 6(a), respectively. There is a clear enhancement of the peaks at the point at which their emission

wavelengths are overlapped ($\lambda_p \sim 1960$ nm), and significant enhancement of the combined peak [$\sim 40\%$ larger than predicted; see the blue dashed line] indicating the production of a stimulated SRR. Figure 6(c) shows the phase-matching curves of all of the radiations in diamond for $\lambda_p = 1960$ nm. Backward RR (the green dashed line) is unimportant since it would be phase matched at very short wavelengths (106 nm). The THRR is predicted at 390 nm, overlapping with the fifth harmonic, as seen in the experiment. Phase-matching curves are not straight lines due to the strong contribution of the shock term for high intensities and normal dispersion; see Ref. [27]. The conversion efficiency from the pump pulse to the SRR peak is estimated to be $\sim 10^{-5}$ due to the short propagation distance and the rapid intensity drop in normal dispersion. However, this is an important proof of concept of the SRR formation, which is open to improvements once the appropriate materials and waveguides that are able to phase match SRR over long distances are found.

Conclusions.—We have shown that the THRR can be stimulated by a higher harmonic when the two are spectrally close. The resonant radiation peak could grow indefinitely in a stimulated fashion, with its amplitude even becoming *higher* than the pump itself in some cases. We have seen experimentally some preliminary hints of SRR in diamond, where a very intense pulse propagates in normal dispersion and the radiation is stimulated by the fifth harmonic. Our findings could lead, by using appropriate waveguides or bulk crystals, to superefficient frequency conversion effects.

-
- [1] J. N. Elgin, T. Brabec, and S. M. J. Kelly, *Opt. Commun.* **114**, 321 (1995).
 - [2] N. Akhmediev and M. Karlsson, *Phys. Rev. A* **51**, 2602 (1995).
 - [3] A. V. Husakou and J. Herrmann, *Phys. Rev. Lett.* **87**, 203901 (2001).
 - [4] F. Biancalana, D. V. Skryabin, and A. V. Yulin, *Phys. Rev. E* **70**, 016615 (2004).
 - [5] D. V. Skryabin *et al.*, *Science* **301**, 1705 (2003).
 - [6] M. Erkintalo, G. Genty, and J. M. Dudley, *Opt. Lett.* **35**, 658 (2010).
 - [7] M. Durand, A. Jarnac, A. Houard, Y. Liu, S. Grabielle, N. Forget, A. Durécu, A. Couairon, and A. Mysyrowicz, *Phys. Rev. Lett.* **110**, 115003 (2013).
 - [8] M. Durand, K. Lim, V. Jukna, E. McKee, M. Baudelet, A. Houard, M. Richardson, A. Mysyrowicz, and A. Couairon, *Phys. Rev. A* **87**, 043820 (2013).
 - [9] T. Roger, D. Majus, G. Tamosauskas, P. Panagiotopoulos, M. Kolesik, G. Genty, I. Gražulevičiūtė, A. Dubietis, and D. Faccio, *Phys. Rev. A* **90**, 033816 (2014).
 - [10] M. Conforti, F. Baronio, and S. Trillo, *Phys. Rev. A* **89**, 013807 (2014).
 - [11] C. Millián and D. V. Skryabin, *Opt. Express* **22**, 3732 (2014).
 - [12] S. Coen, H. G. Randle, T. Sylvestre, and M. Erkintalo, *Opt. Lett.* **38**, 37 (2013).

- [13] J. K. Jang, M. Erkintalo, S. G. Murdoch, and S. Coen, *Opt. Lett.* **39**, 5503 (2014).
- [14] M. R. E. Lamont, Y. Okawachi, and A. L. Gaeta, *Opt. Lett.* **38**, 3478 (2013).
- [15] Y. Okawachi, K. Saha, J. S. Levy, Y. Henry Wen, M. Lipson, and A. L. Gaeta, *Opt. Lett.* **36**, 3398 (2011).
- [16] S. Malaguti, M. Conforti, and S. Trillo, *Opt. Lett.* **39**, 5626 (2014).
- [17] M. Conforti, A. Marini, T. X. Tran, D. Faccio, and F. Biancalana, *Opt. Express* **21**, 31239 (2013).
- [18] P. Kinsler, *J. Opt. Soc. Am. B* **24**, 2363 (2007).
- [19] E. Rubino, J. McLenaghan, S. C. Kehr, F. Belgiorno, D. Townsend, S. Rohr, C. E. Kuklewicz, U. Leonhardt, F. König, and D. Faccio, *Phys. Rev. Lett.* **108**, 253901 (2012).
- [20] Sh. Amiranashvili, U. Bandelow, and N. Akhmediev, *Phys. Rev. A* **87**, 013805 (2013); Sh. Amiranashvili and A. Demircan, *Adv. Opt. Technol.* **2011**, 989515 (2011).
- [21] C. Redondo Loures, A. Armaroli, and F. Biancalana, *Opt. Lett.* **40**, 613 (2015).
- [22] C. Redondo Lourés, D. Faccio, and F. Biancalana, *Phys. Rev. Lett.* **115**, 193904 (2015).
- [23] J. McLenaghan and F. König, *New J. Phys.* **16**, 063017 (2014).
- [24] F. Biancalana, *Physics* **5**, 68 (2012).
- [25] A. Demircan, S. Amiranashvili, C. Brée, and G. Steinmeyer, *Phys. Rev. Lett.* **110**, 233901 (2013).
- [26] A. Demircan, S. Amiranashvili, C. Brée, U. Morgner, and G. Steinmeyer, *Opt. Express* **22**, 3866 (2014).
- [27] T. Roger, M. F. Saleh, S. Roy, F. Biancalana, C. Li, and D. Faccio, *Phys. Rev. A* **88**, 051801 (2013).
- [28] B. Zhou, H. Guo, and M. Bache, *Phys. Rev. A* **90**, 013823 (2014).
- [29] B. Zhou *et al.*, arXiv:1606.00572.